EUROPEAN SYNCHROTRON RADIATION FACILITY

INSTALLATION EUROPEENNE DE RAYONNEMENT SYNCHROTRON

ESRF

# Experiment Report Form

**The double page inside this form is to be filled in by all users or groups of users who have had access to beam time for measurements at the ESRF**.

Once completed, the report should be submitted electronically to the User Office via the User Portal:

*https://wwws.esrf.fr/misapps/SMISWebClient/protected/welcome.do*

***Reports supporting requests for additional beam time***

Reports can be submitted independently of new proposals – it is necessary simply to indicate the number of the report(s) supporting a new proposal on the proposal form.

The Review Committees reserve the right to reject new proposals from groups who have not reported on the use of beam time allocated previously.

***Reports on experiments relating to long term projects***

Proposers awarded beam time for a long term project are required to submit an interim report at the end of each year, irrespective of the number of shifts of beam time they have used.

***Published papers***

All users must give proper credit to ESRF staff members and proper mention to ESRF facilities which were essential for the results described in any ensuing publication. Further, they are obliged to send to the Joint ESRF/ ILL library the complete reference and the abstract of all papers appearing in print, and resulting from the use of the ESRF.

Should you wish to make more general comments on the experiment, please note them on the User Evaluation Form, and send both the Report and the Evaluation Form to the User Office.

## Deadlines for submission of Experimental Reports

- 1st March for experiments carried out up until June of the previous year;
- 1st September for experiments carried out up until January of the same year.

## Instructions for preparing your Report

- fill in a separate form for each project or series of measurements.
- type your report, in English.
- include the reference number of the proposal to which the report refers.
- make sure that the text, tables and figures fit into the space available.
- if your work is published or is in press, you may prefer to paste in the abstract, and add full reference details. If the abstract is in a language other than English, please include an English translation.

| | | |
|---|---|---|
| ESRF | **Experiment title:** Solution structure of the complex between human 14-3-3 protein and phosphorylated small heat shock protein HSPB6 (HSP20). | **Experiment number**: MX-1663 |
| **Beamline**: BM29 | **Date of experiment**: from: 09/12/2014 to: 10/12/2014 | **Date of report**: 25/02/2015 |
| **Shifts:** 2 | **Local contact(s)**: Emilie POUDEVIGNE, Martha BRENNICH | *Received at ESRF:* |


**Names and affiliations of applicants** (* indicates experimentalists):

Alexander SHKUMATOV*, Dmytro GUZENKO*, Sergei STRELKOV

Laboratory for Biocrystallography, Department of

Pharmaceutical and Pharmacological Sciences

O&N2, Campus Gasthuisberg, KU Leuven,

Herestraat 49, 3000 Leuven, Belgium


## Report:

Small Heat Shock Proteins (sHSPs) are ubiquitous family of ATP-independent chaperones. They bind partially denatured proteins, thereby preventing irreversible protein aggregation during stress. A typical sHSP monomer consists of a distinct conserved β-sandwich domain named the α-crystallin domain (ACD), forming dimers, whereby the termini are flexible, vary in length and lack sequence conservation across different species. The variable amino- and carboxy-terminal extensions are thought to direct the formation of larger sHSP oligomers, however, the exact mechanism, determinants of oligomerization and even exact oligomer state are still elusive. Recently, using a hybrid approach for structural and functional investigation of human HSPB6, we obtained insights into structure and dynamics of this dimeric protein by combining partial crystallographic structures and SAXS data [1]. Phosphorylated HSPB6 have a specific site for interaction with 14-3-3 proteins - well-known universal adaptors participating in multiple vital cellular processes due to their ability to recognize phosphorylated partner proteins. The main aim of this project was to provide a comprehensive structural picture of 14-3-3/HSPB6 complex and its constituents in solution using available partial crystal structures and SAXS data. Moreover, as a pilot experiment we performed SAXS measurements using few chimeric HSPs to understand better mechanism and determinants of oligomerization.

During the ESRF visit, we performed SAXS measurements of a C-terminal deletion mutant of HSPB6, a deletion mutant of 14-3-3, their complex as well as complexes with two other mutants of HSPB6, where 10 residues were removed from N-terminal region (HSPB6.Δ21-30 and HSPB6.Δ31-40). In 2013 we performed SAXS measurements at P12 (DESY, Hamburg) in batch mode on full-length complex, however, we could not exclude the possibility of partial complex dissociation. Hence, we also conducted SAXS measurements using an in-line HPLC system (Shodex KW404-4F column). To analyze the HPLC-SAXS results, we developed a tool for a rapid data analysis [2], which provides estimations of forward scattering, *I(0)*, radius of gyration, $R_g$, maximum particle size, $D_{max}$, molecular weight, MW, from Porod volume and volume of correlation of the studied sample as well as outputs a figure reflecting calculated parameters (fig. 1 a,b).

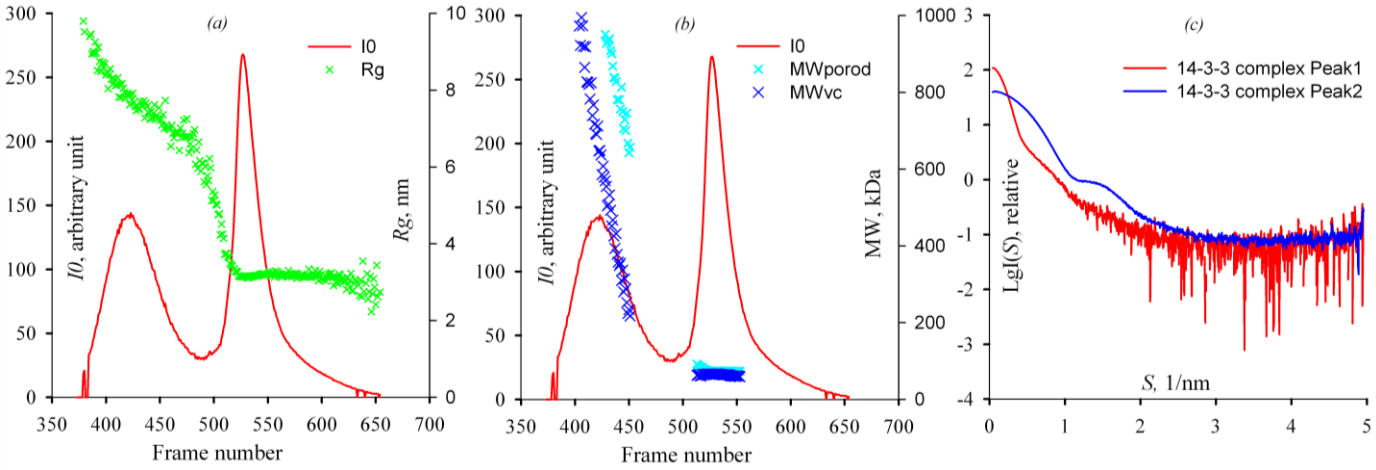


**Figure 1** *(a, b) datasw* output for a 14-3-3 protein complex containing a high molecular weight oligomer (peak 1) alongside with the main species (peak 2). *(c)* SAXS profiles for peak 1 (red line) and peak 2 (blue line).

Subtracted scattering curve for deletion mutant of apo 14-3-3 was extrapolated and further analyzed. There are a number of structures mainly in the peptide-bound closed form but also some in the open form available from PDB. Validation of the scattering data suggested that in solution apo 14-3-3 is present in an open form. Our previous data on 14-3-3 bound to a peptide suggested a closed conformation consistent with the published results [3].

We then compared the extrapolated scattering curve obtained from the concentration series of 14-3-3/HSPB6 complex recorded in the batch mode with the peak#2 average from HPLC-SAXS, showing an excellent agreement, despite an additional peak (#1) seen in HPLC profile (fig. 1). This additional peak, representing high MW oligomers, could have resulted from a rather high loaded concentration in HPLC mode (~12.5 mg/ml) or unspecific interaction of the sample with the column.

The extrapolated data was further analyzed and used for model validation. MW estimation confirmed expected 2:2 stoichiometry of the complex. The available partial structure of HSPB6 represents ACD, whereas most of the ~70 residues N-terminal are presumably dynamic. We used the program CORAL to build the missing residues while dimeric ACD and 14-3-3 were treated as rigid bodies with the former allowed to move freely.

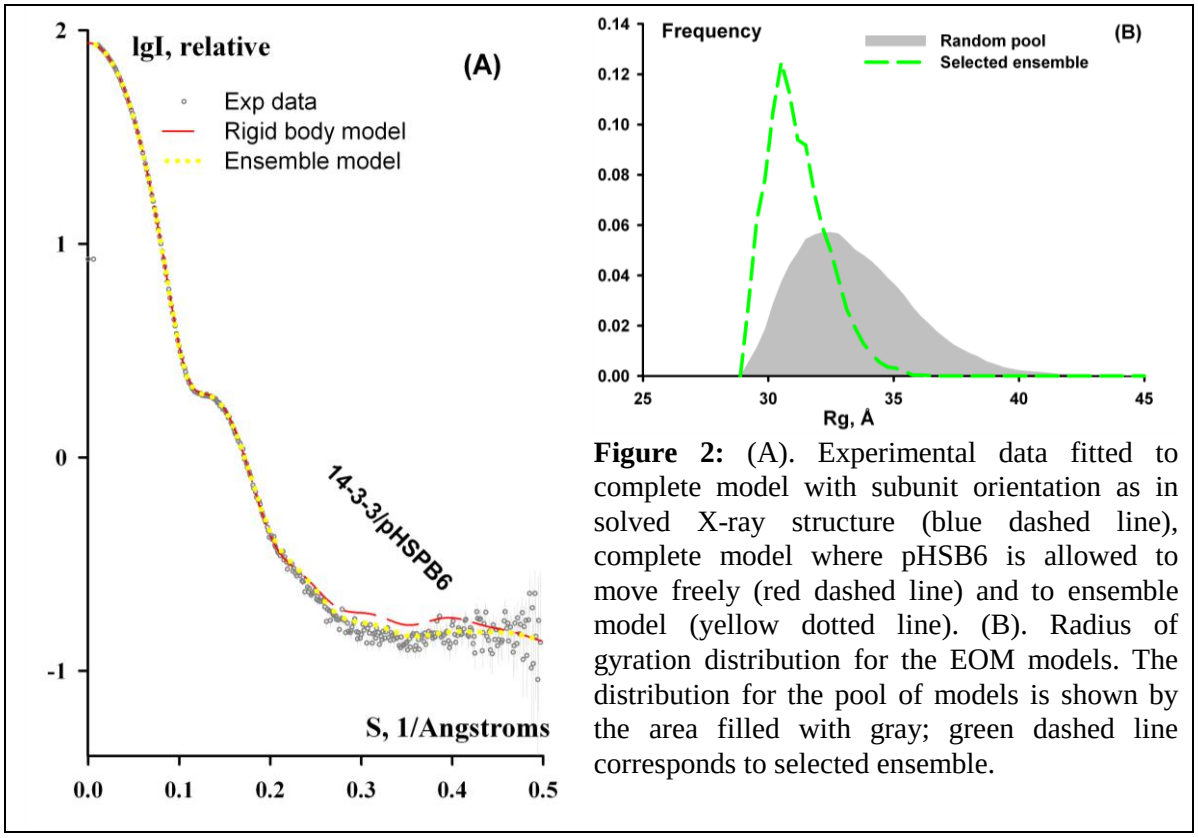


**Figure 2:** (A). Experimental data fitted to complete model with subunit orientation as in solved X-ray structure (blue dashed line), complete model where pHSB6 is allowed to move freely (red dashed line) and to ensemble model (yellow dotted line). (B). Radius of gyration distribution for the EOM models. The distribution for the pool of models is shown by the area filled with gray; green dashed line corresponds to selected ensemble.

The resulting models ('Rigid body model') could not reconstitute the scattering data very well (table 1, fig. 2A) and there was no convergence observed with HSPB6 being positioned in different orientations with respect to 14-3-3 in 20 different CORAL reconstructions. Kratky plot suggested a rather compact arrangement of all complexes (data not shown), however no interaction interface was determined for both proteins, implying that the N-terminal part of HPSB6, bearing sequence identical to peptides binding 14-3-3, could be harnessed by 14-3-3 protein, allowing for multiple conformations present simultaneously in solution. Hence we performed ensemble analysis using ensemble optimization method (EOM). EOM is limited to single chain proteins only. To overcome this limitation and given the proximity of the C-terminus of 14-3-3 to the N-terminus of HPSB6, the sequences were united, whereas the sequence in their symmetry mates was inversed to mimic a single chain. Using available partial structures and a pseudo-sequence, program RANCH was used to generate 10,000 models for each possible scenario (dihedral angle distributions) of modeling missing parts: compact chain (CC), native-like (NL) and random coil (RC). The position of 14-3-3 was fixed together with peptides in the peptide binding sites of 14-3-3 and only symmetric part of HPSB6 – dimeric alpha-crystallin domain (ACD) – was allowed to move, while missing N-terminal linkers were modeled. Thereafter a genetic algorithm, GAJOE, was used to select an ensemble model based on the available SAXS data. Each individual RANCH model was also fitted to the scattering data. GAJOE was run 10 times to ensure reproducibility and convergence of the obtained results. Ensemble modeling resulted in a converging solution in terms of distribution of Radius of gyration ($R_g$) and a more narrow range of discrepancy (fig. 2b, table 1). Interestingly, the lowest discrepancy was observed for CC scenario (table 1), suggesting also that the selected ensemble should have a very compact preferred arrangement (fig. 2b), whereby HSPB6 would have multiple orientations with respect to the cleft-side of the 14-3-3. This result is in-line with our previous observations, that N-terminus of HSPB6 is flexible but within a rather confined area [1]. The discrepancy could further be improved using an all-atom ensemble modeling pipeline (FULCHER) developed in our group (table 1) [4]. The subsequent refinement using normal modes of top scoring 5,000 all-atom models, according to MolProbity clash score, did not improve significantly discrepancy. This, however, indicated that reasonable fitting of scattering data can be achieved even with top scoring stereochemically sound models present in the random pool.

**Table 1**: SAXS modelling summary.

| **Combined ab initio/rigid body modeling with CORAL** | | | |
|---|---|---|---|
| | HSPB6 free | | |
| **Chi^2 range** | 2.28-6.07 | | |
| **Ensemble modeling with EOM** | | | |
| | CC | NL | RC |
| **Chi^2 range for ensemble** | 2.56-2.69 | 2.942-3.058 | 2.760-3.016 |
| **Chi^2 range for single model** | 3.15-3285.67 | 2.90-3418.4 | 2.61-3673.30 |
| **All-atom modeling with FULCHER** | | | |
| **Chi^2 range for ensemble** | 2.46- 2.51 | - | - |
| **Chi^2 range for single model** | 2.39-3173.61 | - | - |
| **NMA-refined all-atom models (5 Angstroms amplitude)*** | | | |
| **Chi^2 range for ensemble** | 2.48-2.63 | - | - |
| **Chi^2 range for single model** | 2.39-3228.65 | - | - |

* Half of all-atom models according to MolProbity clash score were used for NMA-based refinement.

The scattering data for the other two complexes was analyzed in a similar manner, although EOM analysis was not possible due to presence of flexible C-terminus in HSPB6 constuct, making it impossible to unite sequences in a single pseudochain. For both constructs, generated CORAL models showed different position and orientation of HSPB6 with respect to 14-3-3 with Chi^2 ranging from 4.62 to 8.64 and 2.16 to 4.73 for 14-3-3/HSPB6.d21-30 and 14-3-3/HSPB6.d31-40, respectively.

As a pilot project we measured chimeras with C-terminal domain swap of HSPB6 (named '665') and N-terminal domain swap of HSPB5 ('655') as well as wild type proteins, present in solution as a dimer (HSPB6) and a ~24-mer (HSPB5). We expected that both constructs would behave like dimeric HSPB6.WT, as we believe that N-terminal region of HSPB6 could govern the oligomerization or more precisely its absence (ACD dimer in solution is present as a dimer). However, the analysis of HPLC-SAXS data for both constructs revealed fibrillation-like behaviour (fig. 3), which is neither observed for HSPB6 nor for HSPB5. Fibrils seem to have a similar cross section (analysis is in progress) and grow with the increasing concentration as judged from increase of $D_{max}$ with increasing concentration for data recorded in the batch

mode. Currently, we are preparing several other constructs, among which the most important ones have a C-terminal domain swap of HSPB5 (556) and ACD domain swaps (656 and 565). This will allow us to pinpoint the main determinants of oligomerization and understand if the domain/region crosstalk is required for correct oligomerization behaviour.

**Figure3:** HPLC-SAXS analysis of 665 (A, B) and 655 (C, D).

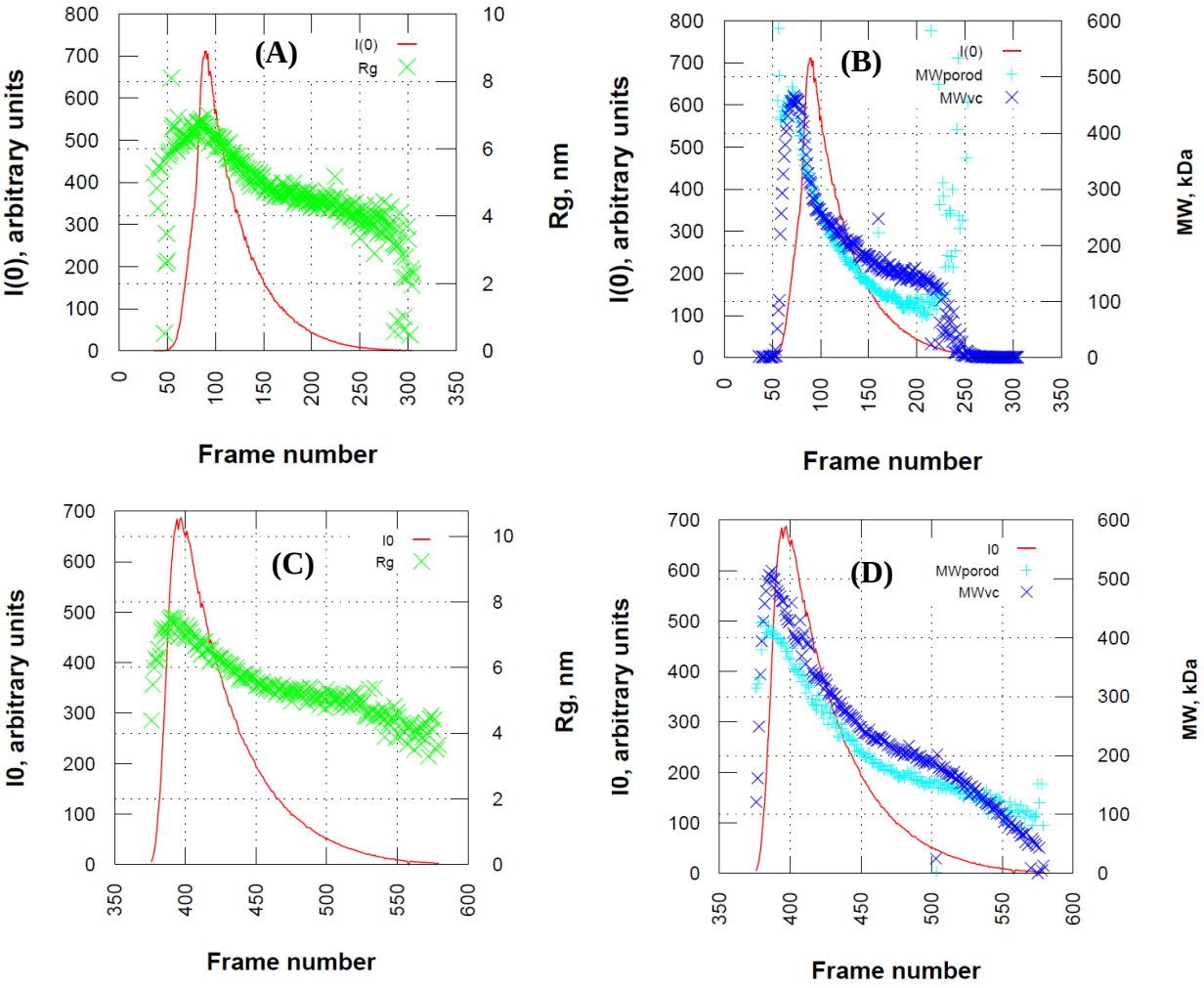


## References:


[1] Weeks, S.D., Baranova, E.V., Heirbaut, M., Beelen, S., Shkumatov, A.V., Gusev, N.B., Strelkov, S.V. (2014) Molecular structure and dynamics of the dimeric human small heat-shock protein HSPB6. Journal of Structural Biology 185: 3. 342-354

[2] Shkumatov, A.V., Strelkov, S.V. (2015) datasw, a tool for HPLC-SAXS data analysis. Acta Crystallographica Section D. *Under review.*

[3] Yang X, Lee WH, Sobott F, Papagrigoriou E, Robinson CV, Grossmann JG, Sundström M, Doyle DA, Elkins JM. (2006). Structural basis for protein-protein interactions in the 14-3-3 protein family. Proc Natl Acad Sci U S A. 2006 Nov 14;103(46):17237-42

[4] Shkumatov, A.V. et al. *In Preparation.*